Plasma Science and Technology

PAPER

Diagnostics of laser-induced plasma on carbon-based polymer material using atomic and molecular emission spectra

To cite this article: Jelena PETROVIĆ *et al* 2023 *Plasma Sci. Technol.* **25** 045507

Plasma Sci. Technol. **25** (2023) 045507 (9pp) https://doi.org/10.1088/2058-6272/aca30f

Diagnostics of laser-induced plasma on carbon-based polymer material using atomic and molecular emission spectra

Jelena PETROVIĆ[1], Dragan RANKOVIĆ[2,*], Miroslav KUZMANOVIĆ[2], Jelena SAVOVIĆ[1], Vasili KIRIS[3], Alena NEVAR[3], Mikhail NEDELKO[3] and Nikolai TARASENKO[3]

[1] University of Belgrade, Institute of Nuclear Sciences Vinca, Mike Petrovica Alasa 12-14, Belgrade 11001, Serbia
[2] University of Belgrade, Faculty of Physical Chemistry, Studentski trg 12-16, Belgrade 11000, Serbia
[3] Institute of Physics, National Academy of Sciences of Belarus, Nezalezhnasci Ave. 68-2, Minsk 220072, Belarus

E-mail: dragan@ffh.bg.ac.rs

Received 16 August 2022, revised 14 November 2022
Accepted for publication 15 November 2022
Published 8 February 2023

Abstract

Time-integrated optical emission analysis of laser-induced plasma on Teflon is presented. Plasma was induced under atmospheric pressure air using transversely excited atmospheric CO_2 laser pulses. Teflon is a C-based polymer that is, among other things, interesting as a substrate for laser-induced breakdown spectroscopy analysis of liquid samples. This study aimed to determine the optimal experimental conditions for obtaining neutral and ionized C spectral lines and C_2 and CN molecular band emission suitable for spectrochemical purposes. Evaluation of plasma parameters was done using several spectroscopic techniques. Stark profiles of appropriate C ionic lines were used to determine electron number density. The ratio of the integral intensity of ionic-to-atomic C spectral lines was used to determine the ionization temperature. A spectral emission of C_2 Swan and CN violet bands system was used to determine the temperature of the colder, peripheral parts of plasma. We critically analyzed the use of molecular emission bands as a tool for plasma diagnostics and suggested methods for possible improvements.

Keywords: spectroscopy of laser-induced plasma, laser-induced breakdown spectroscopy, transversely excited atmospheric CO_2 laser, plasma diagnostics, atomic and molecular emission spectra, Teflon

(Some figures may appear in colour only in the online journal)

1. Introduction

Laser-induced breakdown spectroscopy (LIBS) is an atomic spectroscopy technique suitable for fast elemental analysis of various types of samples [1, 2]. The analytical potential of LIBS also includes the analysis of different organic materials, such as biological specimens [3, 4], polymers [5–7], and traces of explosives [8–10]. LIBS spectra of organic compounds can be fairly complex due to the simultaneous presence of atomic and ionic emission lines and molecular emission bands [11]. In addition, the registered intensity and features of both the atomic lines and molecular bands are influenced by many experimental parameters. Depending on the applied laser radiation (wavelength, pulse duration, irradiance), the surrounding atmosphere, and the signal detection mode (time-gated or time-integrated), the registered spectral signature of organic material may be quite different [12]. It should be noted that, due to the difference in the excited-state lifetimes of atoms and molecules, experimental conditions can be adjusted so that the spectra are dominated either by atomic or molecular emission lines.

* Author to whom any correspondence should be addressed.

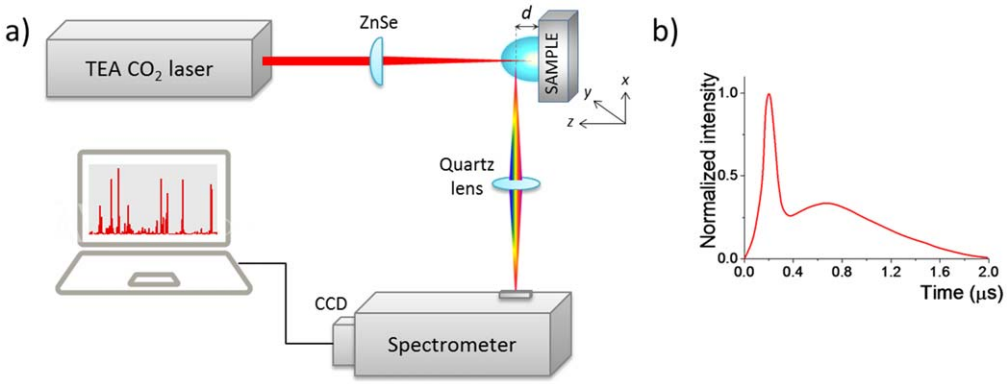

Figure 1. LIBS experimental setup based on a TEA CO_2 laser (a) and temporal profile of the TEA CO_2 laser pulse (b).

This work used a laboratory LIBS setup based on a transversely excited atmospheric (TEA) CO_2 laser and time-integrated spatially resolved detection of spectral emission to study Teflon plasma. The relevance of research on laser plasma induced on Teflon is twofold. The first relates to using Teflon as a substrate for LIBS analysis of solutions [13, 14]. For this purpose, a micro drop of solution is first applied to the surface of Teflon and dried, after which the laser irradiates the dried spot and induces plasma. The suitability of Teflon as a substrate lies in its chemical inertness and chemical purity. Teflon is a fluorocarbon-based polymer. Because of the high excitation energy of F, the possible spectral interferences are limited to C, i.e., the LIBS spectrum is mainly dominated by spectral lines of the deposited material. The second is that Teflon results are relevant for LIBS analysis of different organic materials, emphasizing polymers characterized by high C content and solely composed of non-metal elements. One must be aware that laser-induced plasma is more challenging to obtain on polymers than on most other materials due to the high ionization energy and covalent bonding. The present research is focused on optimizing the conditions to obtain plasma suitable for spectrochemical application and developing appropriate spectral methods for Teflon plasma diagnostics, i.e., determination of plasma parameters.

LIBS plasma induced on the Teflon target emitted strong C lines (C I and C II) and bands of C_2 and CN molecules, suitable for plasma diagnostics. We used a Stark profile of the C II line to evaluate the electron number density. The ionization temperature was calculated using the two-line ratio method. Emission of C_2 and CN molecular bands was used to estimate the rotational (T_{rot}) and vibrational (T_{vib}) temperatures.

2. Experiment

The LIBS setup shown in figure 1 has been described in detail elsewhere [15], and we will briefly recall its main characteristics.

The excitation source for LIBS was a TEA CO_2 laser with emission in the mid-infrared spectral region (10.6 μm) with variable pulse energy up to 170 mJ/pulse and a maximum frequency of 2 Hz, operating in a multimode regime. A pulse is composed of a peak (FWHM = 120 ns) followed by a μs-tail of lower intensity. About 35% of the pulse energy is contained in the initial spike. A laser beam was focused on the target mounted on the translational stage, using a ZnSe lens with a focal length of 13.0 cm. The laser beam was focused on the Teflon plate (2 mm thickness) that had been previously polished with sandpaper (2000 grit) and cleaned with ethyl alcohol. The angle of the laser beam was ~90°. The beam cross-section has a quadratic form with uniform intensity distribution. The area of the created spot on the sample surface was 0.014 cm^2 for a beam focused 5 mm in front of the Teflon target. The plasma emission was projected onto the entrance slit of the PGS-2 (Carl Zeiss) monochromator using an achromatic quartz lens with a focal length of 273 mm. The slit width was 50 μm, and the height was 2 mm. A charge-coupled device (CCD) Apogee Alta F1007 camera was used for signal detection. The camera consists of 1024 × 122 pixels, each pixel of which is 12 μm × 12 μm, with an active area of 12.3 mm × 1.46 mm. The camera has a high quantum efficiency in the ultraviolet and visible light spectral regions. The dispersion was about 7 nm mm^{-1}, and the typical resolution was 0.027 nm. For the applied spectral dispersion, a spectral range of 9 nm was recorded in a single acquisition.

Unless otherwise stated, experiments were conducted using a laser pulse energy of 150 mJ with the beam focused 5 mm in front of the target surface. The corresponding fluence was 10 J cm^{-2}, while the peak power density was 35 MW cm^{-2}. Time-integrated spatially resolved LIBS spectra were obtained by recording the optical emission from a plasma slice at a selected distance (d) from the target. Selection of a viewing plasma region was obtained by moving the target along the plasma expansion direction (z-axis in figure 1) while keeping a constant distance between the focusing lens and the target. In this way, the effect of eliminating the initial emission of the continuum was achieved, similar to the spatially integrated time-resolved measurements. The spectra were acquired using a time-integrated mode for signal detection, with a typical integration time of 20 s. Therefore, 20 consecutive laser pulses were accumulated from different locations on the sample. Measurements were repeated three times, and the resulting LIBS spectra were averaged. Low dark current noise gives a better signal-to-noise ratio (SNR) for a longer integration time compared to

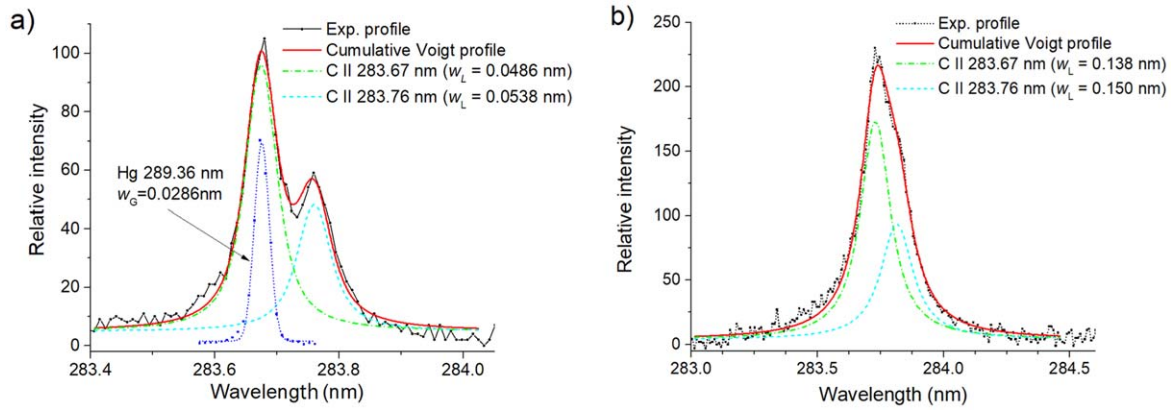

Figure 2. Profiles of C II lines emitted from Teflon plasma. The laser energy was 150 mJ. The beam was focused 5 mm in front of the target. Time-integrated emission spectra were recorded at 0.9 mm (a) and 0.3 mm from the target (b). Note that in (a), the *x*-axis does not apply to the Hg line, which was shifted for clarity. w_L and w_G are the Lorentzian and Gaussian widths of the profile distribution.

Table 1. Parameters of C lines relevant for plasma diagnostics for given values of temperature and electron number density: electron impact width (w) and shift (D) [16]; excitation energy (E_{exc}), and a product of transition probability and a statistical weight ($A{\cdot}g$) [17].

C lines (nm)	w (nm) $T = 10^4$ K,	D (nm) $N_e = 10^{17}$ cm^{-3}	w (nm) $T = 2 \times 10^4$ K,	D (nm) $N_e = 10^{17}$ cm^{-3}	E_{exc} (eV)	$A{\cdot}g$ (10^8 s^{-1})
C I 247.86	0.361×10^{-2}	0.438×10^{-2}	0.417×10^{-2}	0.477×10^{-2}	7.68	8.4
C II 283.67	0.928×10^{-2}	0.724×10^{-2}	0.767×10^{-2}	0.573×10^{-2}	16.33	13.2
C II 283.76	—	—	—	—	16.33	6.58
C II 250.91	—	—	—	—	18.65	1.88
C II 251.21	—	—	—	—	18.65	3.37

individual registration of each pulse, with subsequent averaging, due to the multiplication of reading noise.

3. Results and discussion

3.1. Determination of electron number density

The high emission intensity of C atomic and ion lines and C_2 and CN molecular bands from Teflon plasma makes them suitable for plasma diagnostics. In laser-induced plasmas, due to relatively high electron number densities (N_e) and a measurable quadratic Stark effect for many elements, a suitable method for determining N_e is by measuring Stark profiles of spectral lines. A particular convenience of this method is that it does not require any assumptions regarding local thermodynamic equilibrium. Under typical LIBS plasma conditions, the most intense C lines are C I 247.86 nm and C II 283.67 nm. Except for in the plasma core, the atomic line at 247.86 nm is generally much more intense than ionic C lines and suited for plasma diagnostics under a wide range of temperature and electron density values. However, for the same electron density, the C II 283.67 nm ionic line has an around two times wider line profile than the atomic line (table 1), reducing the requirement for the spectral resolution of the spectrograph. The symmetry of ionic lines and the asymmetry of the profile of atomic lines is an additional advantage of the utilization of ionic lines for the determination of N_e because determining the half-width of the symmetric line profile by fitting is easier and more accurate. Depending on the FWHM of the instrumental profile and the electron density, the application of C II 283.67 nm for plasma diagnostics could be limited by partial overlap of the adjacent C II 283.76 nm line. On the other hand, because they have the same excitation energy, the intensity ratio of these two lines is independent of temperature, making deconvolution easier.

Figure 2(a) shows the profile of C II spectral lines. The figure also shows a profile of the Hg I 289.36 nm line (emitted from a Hg pen lamp under low pressure) that we used to determine the instrumental profile. The Hg spectral line has a very narrow physical profile (due to the low pressure and low gas temperature) which can be neglected even compared to the instrumental profile of high-resolution spectrometers. In the peak deconvolution procedure, the approximate positions of both lines were entered, and the Gaussian components (w_G) of both profiles were fixed, equalizing them with the instrumental profile (0.028 nm for the applied slit width of 25 μm). As a result of a deconvolution procedure, approximately the same Lorentz half-widths (w_L) were obtained for both lines (0.055 nm and 0.056 nm, respectively). The intensity ratio of the peaks (1.95) is in excellent agreement with the ratio of their $A{\cdot}g$ values (2.01), which is clear evidence of the accuracy of the applied deconvolution procedure. The distance between the peaks ($\Delta\lambda = 0.093$ nm) is in good agreement with the difference in their tabulated wavelengths ($\Delta\lambda = 0.089$ nm), indicating that both C lines, 283.76 nm

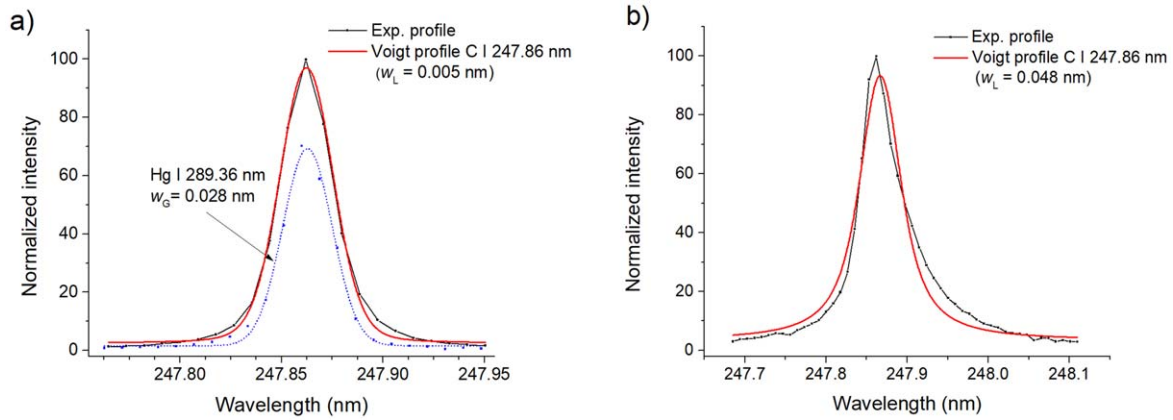

Figure 3. Profile of an atomic C I 247.86 nm line emitted from Teflon plasma. Time-integrated emission spectra from a plasma slice at 0.9 mm (a) and 0.3 mm from the target (b). Note that in (a), the *x*-axis does not apply to the Hg line, which was shifted for clarity.

and 283.67 nm, have approximately the same widths and shifts.

The C ionic lines recorded at distances closer to the target ($d = 0.3$ mm) are suitable for diagnostics of denser and hotter plasma, as demonstrated in figure 2(b). Although the profiles significantly overlap, and without fixing the distance between the peaks, the obtained peaks still fit well with the assumed distance between them (0.085 nm) and their theoretical intensity ratio (1.80). The obtained Lorentzian profile widths of both lines (0.138 nm and 0.150 nm) match each other by 10%. More accurate deconvolution results could be obtained by fixing the same expected value of the Lorentzian component for both profiles and the position of a lower-intensity peak using a tabulated value of a distance from the higher-intensity peak. When applied, the described procedure would give the intensity ratio of the peaks of 2.02 and the Lorentz width of 0.137 nm for both lines.

The electron number density (in cm^{-3}) can be inferred from Stark broadening tables [16] using the relation:

$$\Delta\lambda = 2w\frac{N_e}{10^{17}} \tag{1}$$

The obtained FWHM of the C II 283.67 nm line profile was from 0.150 to 0.030 nm, depending on the observation distance relative to the target surface. The corresponding electron number densities were in the range of 1.9×10^{17}–$9.4 \times 10^{17}\,\mathrm{cm}^{-3}$. This range is almost identical to the applicability range of the 283.67 nm line for determining N_e. The deconvolution error increases for higher electron number densities because of the increased extent of line overlapping. On the other hand, for electron densities less than $10^{17}\,\mathrm{cm}^{-3}$, C ionic lines are of low intensity and difficult to detect. An additional problem at lower electron concentrations is the width of the Stark profile of the 283.67 nm line, which becomes comparable to, or smaller than, the instrumental profile of a typical medium resolution spectrometer, which again increases the deconvolution error.

The Stark profile of the atomic C I 247.86 nm line is shown in figure 3 to illustrate why the ionic line 283.67 nm is better suited for determining N_e with a medium resolution spectrometer. As seen in figure 3(a), further away from the target, i.e., in plasma zones of lower electron concentration, the contribution of the Stark broadening to the width of the C I 247.86 nm line is negligible. In other words, the instrumental width determines the FWHM of its experimental profile. Closer to the target (figure 3(b)), the C I 247.86 nm line is asymmetrically broadened, which reduces the fitting procedure quality and increases the N_e determination uncertainty [18].

3.2. Determination of ionization temperature

A pair of C ionic lines around 251 nm and the atomic line at 247.86 nm are suitable for determining the temperature from the ion-to-atom spectral line integral intensities ratio [19]. The C lines used for plasma diagnostics are not resonant. Their lower state energies are high enough (for ionic lines, 13.7 eV and 11.96 eV, and 2.68 eV for the atomic line), so a negligible self-absorption effect can be expected in the temperature range estimated for the applied experimental conditions. The conclusion is supported by the fact that the intensity ratio of the two C II lines (250.91 nm and C II 251.21 nm) obtained under different experimental conditions is close to the ratio obtained using the NIST LIBS application for different temperatures and electron concentrations, which is in agreement with the fact that these two lines have almost identical excitation energy.

These ionic lines are among the most intense C lines. Their intensity ratio does not depend on temperature and can serve as an indicator of the accuracy of intensity measurements. Moreover, they are located near the suitable atomic C line, eliminating the need for calibration of the spectral sensitivity of the spectrometer. It is enough to estimate changes in diffraction grating efficiency and quantum efficiency of a CCD detector in a narrow spectral range of around 250 nm.

The dependence of the ionic-to-atomic line intensity ratios of the same element on plasma temperature and electron density is given by the expression [20]:

$$\frac{I^+}{I^0} = 4.83 \times 10^{15}\frac{g^+A^+\lambda^0}{g^0A^0\lambda^+}\frac{T^{3/2}}{N_e}\mathrm{e}^{-\frac{(E^+_{\mathrm{exc}}+E_{\mathrm{ion}}-\Delta E_{\mathrm{ion}}-E^0_{\mathrm{exc}})\times 11605}{T}} \tag{2}$$

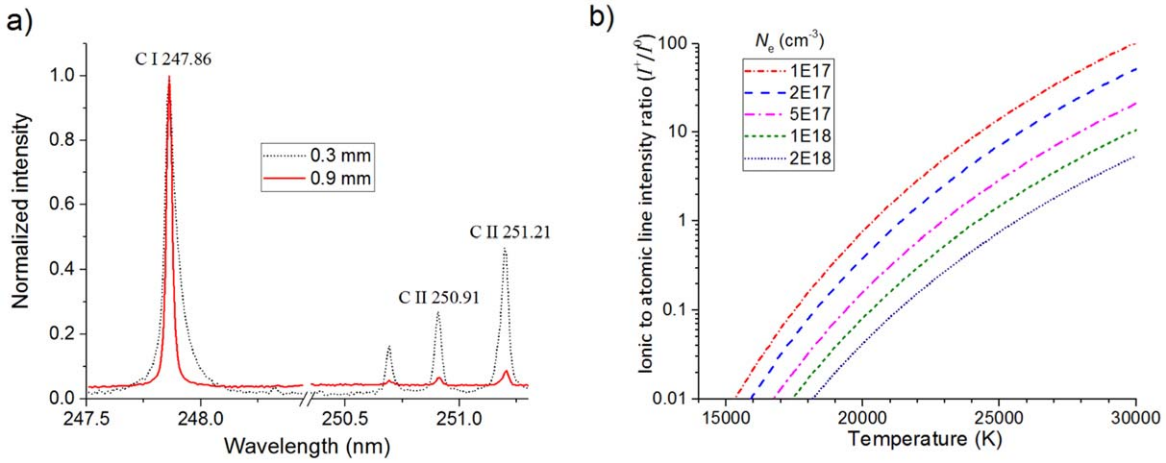

Figure 4. (a) Atomic and ionic spectral lines of C recorded from the plasma zones at $d = 0.3$ mm and 0.9 mm from the target surface. (b) Calculated intensity ratio of ionic-to-atomic intensity ratio (C II 250.91 nm/C I 247.86 nm) as a function of plasma temperature.

where I is the integral intensity of a spectral line; $g{\cdot}A$ is a product of statistical weight and transition probability; λ is the spectral line wavelength; E_{exc} is the excitation potential, E_{ion} is ionization potential, and ΔE_{ion} is the reduction in the ionization potential for the lower ionization state (all expressed in eV); N_e is the electron number density (in cm^{-3}); and and T is the temperature (in K).

The lowering of the ionization energy in plasma is given by:

$$\Delta E_{ion} = 6.95 \times 10^{-7} \times (z+1)^{2/3} \times (N_e)^{1/3} \qquad (3)$$

where $z = 0$ for the ionization of a neutral atom, while the physical constants appearing in equations (2) and (3) have been replaced by their numeric values (in units cm^{-3}, K$^{-3/2}$, and eV).

Figure 4(a) shows spectra acquired from two plasma zones, i.e., from plasma zones at different distances from the target surface ($d = 0.3$ mm and 0.9 mm). In both cases, the intensity ratio of the two ionic lines (251.21 nm and 250.91 nm) matches the ratio of their $g{\cdot}A$ values (1.79) within 2%. Comparing the FWHM of the C lines profile with that of the instrumental profile showed that the Stark broadening is more pronounced for the atomic 247.86 nm line relative to the ionic lines. The square Stark effect makes the 247.86 nm atomic line profile asymmetric. Closer to the target, N_e is higher, resulting in a broader profile of the atomic line, and thus increasing the ionic-to-atomic intensity ratio (figure 4(a)).

Figure 4(b) shows the calculated temperature dependence of the ionic-to-atomic intensity ratio (C II 250.91 nm/C I 247.86 nm) for several N_e values. The experimentally determined ratios of the integral intensities of ionic-to-atomic lines and predetermined N_e values (from the Stark width of the C II 283.67 nm line) were used to calculate the temperature. The estimated ionization temperature was in the range of 16 500 K ($d = 0.9$ mm) to 20 500 K ($d = 0.3$ mm).

The temperature derived from equation (2) is ionic temperature, and the electron density values were obtained from the profile of an ionic C line. With that in mind and considering the spectra acquisition mode (time-integrated, spatially resolved), it is clear that both estimated plasma parameters (T and N_e) characterize the hotter plasma zone and earlier phase of plasma evolution. Since the measurements were not time-resolved, nor was Abel inversion applied, the values obtained are the apparent values of plasma parameters [21]. The obtained values are relevant for the estimation of the excitation properties of the plasma, i.e., for LIBS analytical applications. Nevertheless, the estimated values of the plasma parameters give an insight into the excitation conditions for ion emission and emission of atoms with high ionization energy.

3.3. Evaluation of gas temperature using C_2 and CN molecular band emission

Spectral emission from plasma induced in the air on C-rich materials usually contains intense C_2 and CN molecular bands [22–25]. Both molecules have high dissociation energy, relatively low excitation energy of the first excited electronic state, and favorable transition probability values, all of which contribute to the high intensity of their emission lines. Maximum emission is expected at temperatures of 6200−6500 K. Therefore, the emission spectra of these molecules, primarily bands of the C_2 Swan and CN violet system, are suitable for the diagnostics of colder, peripheral parts of the plasma. Considering the spectral detection method used in this research, as well as the focusing conditions that favor the formation of plasma characterized by high electron concentrations and temperature, the emission from plasma slices closer to the target consists of intense and broadened spectral lines of atoms and ions (from hotter plasma regions) and molecular bands from the peripheral, colder parts of the plasma.

The emission of the Swan system of the C_2 molecule could be registered only from the plasma regions closer to the target. At distances larger than 0.6 mm, the emission intensity was negligible. Such spatial distribution differs from the one obtained for plasma induced on graphite, where the C_2 emission was registered at much larger distances from the

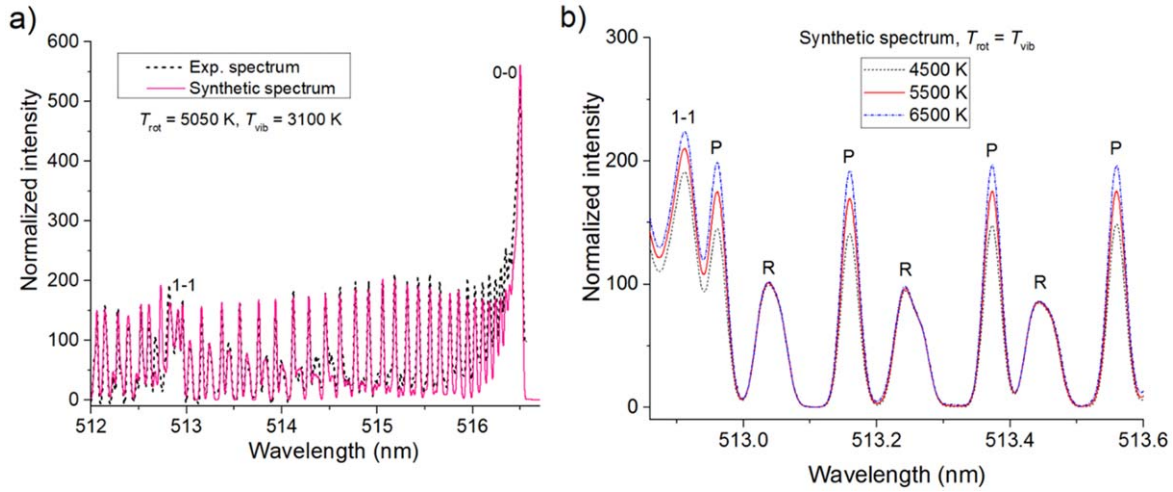

Figure 5. (a) Comparison of the experimental and synthetic spectra of the $\Delta\nu = 0$ sequence of the C_2 Swan system using a laser pulse energy of 160 mJ (focus 5 mm in front of the target; spectra recorded at a distance of 0.3 mm). (b) Enlarged part of the spectrum with indicated positions of the P and R branches.

target. As the C atoms in plasma originate from the target, the reason for this discrepancy is primarily the chemical composition of the Teflon. The C:F molar ratio is $(1/3):(2/3)$. In plasma, F atoms can chemically react with C atoms, creating several chemical species, the most stable of which are CF molecules.

A spectrum of the C_2 Swan (0–0) band was partially superimposed with intense and Stark-broadened ionic spectral lines of N. Because the (0–0) band spectrum cannot be normalized to the intensity of the band head, the rotational temperature (T_{rot}) could not be determined using the entire (0–0) band. A favorable circumstance is that, for the given experimental conditions, the (0–0) band spectrum is sufficiently well resolved (in the region closer to the (1–1) band head), and the *P* and *R* branches are well separated. The theoretical intensity ratio of the *R* component and the (0–0) band head is almost independent of temperature; consequently, the same applies to the relative intensities of the *R* components. Therefore, the rotational lines of the band spectrum can be normalized to the intensity of the R component to avoid problems with band head overlap and self-absorption.

To evaluate the temperature of the peripheral plasma regions from the C_2 molecular spectra, the PGopher program, version 10.0.505, was used. The input file (swan.pgo) was downloaded from the PGopher site (version13 Feb. 2017) [26], with a set of molecular constants taken from [26]. Firstly, the profile width of the experimentally obtained peaks of the P branch was determined using the fact that their components are close in wavelength. The deconvolution showed that the peak profiles were Gaussian, with a half-width almost approximately equivalent to the width of the instrumental profile, 0.027 nm. A comparison of the experimental peak profiles of the R branch with the synthetic profiles generated by the program showed excellent agreement. A defined spectral profile and a roughly approximated value for T_{rot} were used to determine the scaling factors corresponding to the best match between the experimental and synthesized intensities of the R branch peaks. Only the spectrally isolated R peaks from the short-wavelength part of the (0–0) band were considered to avoid the influence of broadened N II lines. In the next step, the value for T_{rot} was adjusted to obtain the best fitting of the P branch peaks in the short-wavelength part of the (0–0) band. The normalized intensity distribution of the portion of the C_2 spectrum lying between the (0–0) and (1–1) band heads is not affected by the value of T_{vib}, which facilitates the fitting procedure and increases its accuracy. The best-fit result was obtained for $T_{rot} = 5100$ K. The band head (1–1) was unsuitable for determining the vibrational temperature. The best-fit result for the predetermined T_{rot} of 5100 K was obtained for $T_{vib} = 3350$ K, figure 5(a). Because of the low sensitivity of the intensity ratio of the (0–0) and (1–1) bands on temperature, the estimated value of T_{vib} is unreliable. Figure 5(b) shows a portion of the spectrum in the (0–0) and (1–1) band regions near the (1–1) band head, to gain more detailed insight into the fitting of the spectrum and its temperature sensitivity.

Comparing the experimental and synthesized (0–0) band head intensities led to the conclusion that the profile and band head intensity are partially perturbed due to self-absorption. Since self-absorption is more pronounced at higher intensities, this was an expected result. Therefore, self-absorption at the most intense band head should always be checked when comparing experimental and synthesized molecular spectra. In any case, avoiding using the most intense band head for normalization is desirable.

The rotational levels have considerably smaller energy intervals than vibrational ones. Thus, the rotational temperature is a more reliable measure of the actual plasma state and corresponds to the gas temperature. Under strong electric or magnetic fields in plasma, the temperatures of electrons and heavy particles can be significantly different, even when plasma is induced under atmospheric pressure. Furthermore,

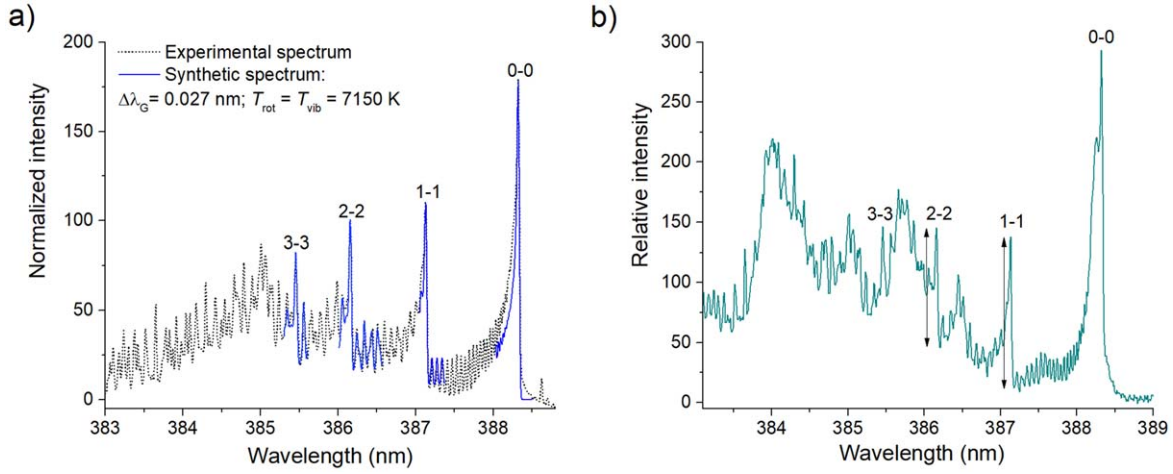

Figure 6. Spectrum of the $\Delta\nu = 0$ sequence of the CN B-X violet system using a laser pulse energy of 160 mJ, recorded at a distance of 0.3 mm (a) and 0.9 mm (b). The beam was focused 5 mm in front of the target.

in the plasma regions where the C_2 molecule is subject to dynamical chemical equilibrium processes (dissociation and the formation of molecules), a significant part of the excited electronic states occurs during the formation of the molecules, making its population distribution sensitive to these chemical processes. In other words, the distribution of some excited states can significantly deviate from the Boltzmann distribution for a given plasma temperature, leading to significant errors in determining the vibrational temperature using the molecular band emission.

Since CN molecules are formed in the interaction of C ablated from the target with ambient air, we can detect intense emission of the $\Delta\nu = 0$ sequence of the B-X violet system up to 2 mm from the target. In the narrow spectral range of 385.5–388.5 nm, there are well separated and intense (0–0), (1–1), (2–2), and (3–3) band heads, which are suitable for determining the vibrational temperature. On the other hand, the rotational structure of the sequence $\Delta\nu = 0$ has no characteristic details suitable for normalizing the spectrum and overcoming the influence of possibly present self-absorption effects. Considering the method used to acquire spectra in this work, an additional problem with the treatment of emission bands of this system is the overlap with the O I, O II, and N II lines. This problem is particularly pronounced in dense and hot plasmas, where the lines of these elements become intense, with significantly broadened profiles due to the Stark effect.

Figure 6(a) shows part of the $\Delta\nu = 0$ sequence of the CN B-X violet system, emitted from a plasma zone of 0.3 mm away from the target, together with the synthesized spectrum obtained for $T_{\mathrm{rot}} = T_{\mathrm{vib}} = 7150$ K and a Gaussian half-width profile of 0.027 nm. By comparing these two spectra, it can be concluded that the experimentally obtained spectrum is superimposed on a broad, symmetrical peak profile (half-width greater than 2 nm) with a maximum of 385.1 nm. It is not easy to precisely determine the origin of this peak. For example, it could be formed by overlapping the highly broadened O II lines (385.08, 385.10, 385.15, and 385.24 nm). Such a spectrum cannot be fitted as a whole with the theoretical spectrum to determine the temperature. However, comparing experimental and synthetic spectra in a very narrow spectral region is possible. The band heads and narrow adjacent parts of the rotational structure around them might be suitable for temperature evaluation. As shown in figure 6(a), for a given temperature of 7150 K, the fitting is excellent for the (2–2) and (3–3), relatively good for the (1–1), and poor for the (0–0) band head. The low-quality peak fitting is probably due to the broadening of the band head profiles caused by the self-absorption effect. The difference in the width of the experimental and synthesized (0–0) band heads, and to a lesser extent the (1–1) band heads, confirms this assumption. Regardless of the self-absorption of the most intense parts of the sequence spectrum, less intense foreheads can be used to estimate the temperature at the plasma periphery.

The influence of the densest and hottest parts of the plasma on the emission of the $\Delta\nu = 0$ sequence from plasma regions further from the target surface is much more pronounced, as shown in figure 6(b). The lines of single charged O (388.22, 388.24, 388.32 nm) are overlapped with the (0–0) band head. The rotational structure is disrupted by a group of broadened lines of single charged C, O, and N ions, which prevents using them for plasma diagnostics. However, some details about the plasma state can be derived from the details of the spectrum. For example, by comparing the intensities of the (1–1) and (2–2) band heads, a temperature of approximately 7200 K was obtained.

The sequence $\Delta\nu = +1$ (figure 7(a)) is of much lower intensity compared to the $\Delta\nu = 0$ sequence and consequently less sensitive to self-absorption. For this sequence, the intensity ratios of the first three band heads are sensitive to changes in temperature, especially the intensity ratios of the (1–0) and (2–1) band heads, as shown in figure 7(b). The ratios of the intensities of the (3–2) and (2–1) band heads increase with increasing temperature up to 6500 K and then decrease with further increasing temperature. The small width of the spectral interval in which these three bands are located is favorable because the spectral sensitivity does not have to

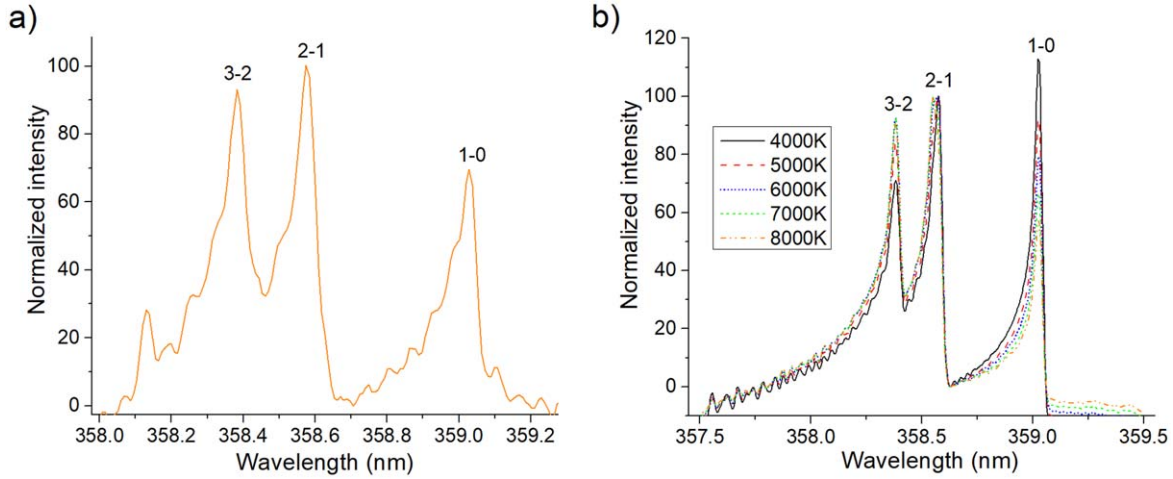

Figure 7. Spectrum of the $\Delta\nu = +1$ sequence of the CN B-X violet system: (a) experimental and (b) synthetic. Experimental conditions were the same as for the spectra shown in figure 5.

be considered. However, the intensity ratios of the band heads of $\Delta\nu = +1$ sequence may be disturbed by overlapping with Stark broadened lines of non-metals, as is the case for the Teflon spectrum. The spectrum shown in figure 7(a) cannot be directly 'overlapped' with the synthesized spectrum. However, from the intensity ratio, a temperature of approximately 6800 K can be roughly estimated.

4. Conclusions

Time-integrated spatially resolved optical emission spectroscopy was applied to study Teflon plasma induced by TEA CO_2 laser pulses. Optimal SNR values of the spectral lines of the C, CN, and C_2 molecular bands were obtained for plasma observed at a distance of 0.3 mm from the target surface. A decreasing trend of SNR values was registered for spectra acquired at higher distances.

Different optical spectroscopy methods were used for plasma characterization. The electron density determined from the Stark width of the C II 283.67 nm line was in the range from $1.9 \times 10^{17}\,\mathrm{cm}^{-3}$ ($d = 0.9$ mm) to $9.4 \times 10^{17}\,\mathrm{cm}^{-3}$ ($d = 0.3$ mm).

The estimated ionization temperature, determined from the C II/C I line ratio, was 16 500 K ($d = 0.9$ mm) to 20 500 K ($d = 0.3$ mm). The obtained plasma parameters characterize the warmer plasma zone and the earlier phase of plasma evolution. However, the estimated values of the plasma parameters provide insight into the excitation conditions for ionic emission and atomic emission of elements with high ionization energy.

A C_2 Swan (0–0) band is unsuitable for estimating the rotational temperature due to the overlapping intense and broad N ion lines. In contrast, P and R components are well resolved in the area closer to the (1–1) band head. The theoretical ratio of intensities of R components and (0–0) band head is almost independent of temperature, and the same applies to the relative intensities of the R components. In order to avoid problems with spectral overlap with the band head and self-absorption, rotational spectral lines can be normalized to the intensity of the R component. The best matching of the experimental with the synthetic spectra was obtained for $T_{\mathrm{rot}} = 5100$ K and $T_{\mathrm{vib}} = 3350$ K. The energy differences of adjacent rotational levels are significantly smaller than the energy differences between adjacent vibration levels. Therefore, the rotational temperature is a much better indicator of the kinetic energy of heavy particles in plasma and describes the gas temperature well.

Intense emission of the $\Delta\nu = 0$ sequence of the CN violet system was detected at a distance up to 2 mm from the target. The best match between the experimental and theoretical spectra for CN molecules was obtained when $T_{\mathrm{rot}} = T_{\mathrm{vib}} = 7150$ K.

The obtained values of plasma parameters are relevant for estimating the excitation properties of the plasma, i.e., for LIBS analytical applications. Apparent values of plasma parameters obtained from C lines describe the central zones of the plasma, while temperatures obtained from the CN and C_2 bands reflect the excitation conditions of the plasma periphery.

Acknowledgments

The research was funded by the Ministry of Education, Science and Technological Development of the Republic of Serbia (Nos. 451-03-68/2022-14/200017 and 451-03-68/2022-14/200146). The Belarusian authors acknowledge the financial support of the State Committee on Science and Technology of the Republic of Belarus and the Belarusian Republican Foundation for Fundamental Research (No. F20SRBG-001).

References

[1] Baudelet M *et al* 2007 *Spectrochim. Acta Part B: At. Spectrosc.* **62** 1329
[2] Fernández-Bravo Á *et al* 2013 *Spectrochim. Acta Part B: At. Spectrosc.* **89** 77

[3] Rehse S J, Salimnia H and Miziolek A W 2012 *J. Med. Eng. Technol.* **36** 77
[4] Zivkovic S *et al* 2017 *Spectrochim. Acta Part B: At. Spectrosc.* **128** 22
[5] Chamradová I, Pořízka P and Kaiser J 2021 *Polym. Test.* **96** 107079
[6] Trautner S *et al* 2017 *Spectrochim. Acta Part A: Mol. Biomol. Spectrosc.* **174** 331
[7] Német B *et al* 1999 *J. Mol. Struct.* **511–512** 259
[8] Abdelhamid M *et al* 2011 *J. Anal. At. Spectrom.* **26** 1445
[9] Lucena P *et al* 2011 *Spectrochim. Acta Part B: At. Spectrosc.* **66** 12
[10] Wang Q Q *et al* 2008 *Spectrochim. Acta Part B: At. Spectrosc.* **63** 1011
[11] Moros J and Laserna J 2019 *Appl. Spectrosc.* **73** 963
[12] Glaus R, Riedel J and Gornushkin I 2015 *Anal. Chem.* **87** 10131
[13] De Giacomo A *et al* 2016 *Anal. Chem.* **88** 5251
[14] Kiris V *et al* 2022 *Spectrochim. Acta Part B: At. Spectrosc.* **187** 106333
[15] Kuzmanovic M *et al* 2019 *Spectrochim. Acta Part B: At. Spectrosc.* **157** 37
[16] Griem H R 1974 *Spectral Line Broadening by Plasmas* (New York: Academic)
[17] Kramida A, Yu R and Reader J 2019 *Team 2013 NIST Atomic Spectra Database*. (Gaithersburg, MD: National Institute of Standards and Technology)
[18] Mijatovic Z *et al* 1993 *J. Quant. Spectrosc. Radiat. Transfer* **50** 329
[19] Petrovic J *et al* 2022 *Plasma Chem. Plasma Process.* **42** 519
[20] Boumans P W J M 1966 *Theory of Spectrochemical Excitation* (New York: Springer)
[21] Aguilera J A and Aragón C 2004 *Spectrochim. Acta Part B: At. Spectrosc.* **59** 1861
[22] Grégoire S *et al* 2012 *Spectrochim. Acta Part B: At. Spectrosc.* **74–75** 31
[23] Hornkohl J O, Parigger C and Lewis J W L 1991 *J. Quant. Spectrosc. Radiat. Transfer* **46** 405
[24] Portnov A, Rosenwaks S and Bar I 2003 *Appl. Opt.* **42** 2835
[25] Western C M 2017 *J. Quant. Spectrosc. Radiat. Transfer* **186** 221
[26] Brooke J S A *et al* 2013 *J. Quant. Spectrosc. Radiat. Transfer* **124** 11